APPLICATION OF POROUS MATERIALS FOR LAMINAR FLOW CONTROL

Wilfred E. Pearce
Douglas Aircraft Company

SUMMARY

The use of porous glove suction panels on the wings of commercial transport aircraft to reduce drag by maintaining laminar flow over the wing surface offers some advantages over alternative methods.

Design studies, wind tunnel testing, and materials and process development work done recently at the Douglas Aircraft Company in Long Beach, California, support the porous glove approach to achieving laminar flow control.

Experimental and development work on porous surfaces to achieve laminar flow has, in the past, received far less attention than the slotted surface alternative. However, the encouraging results achieved so far with porous materials warrant increased activity in this field to expand the data base for practical design purposes.

Douglas, supported by NASA, is continuing design and development on the application of porous materials.

INTRODUCTION

It is well known that laminar flow can be maintained by using suction to remove a small fraction of the boundary layer as its thickness increases in the direction of the flow across the surface.

An obvious advantage of using porous surface material to achieve laminar flow control is that suction can be applied gradually at low velocities normal to the surface, thereby minimizing disturbances and discontinuities within the boundary layer. Also, because the direction of flow within the boundary layer relative to the porous material is not significant, no special orientation is necessary.

With a continuous porous surface, suction air must be ducted from beneath the whole laminar flow control (LFC) surface. A suction glove approach is therefore desirable to avoid a need for multiple holes through the primary supporting structure and to provide a substantial barrier between the air ducting system and the integral fuel tank. This is illustrated in figure 1.

Compared with a slotted system, it offers the advantages of avoiding the difficult problem of machining large numbers of continuous spanwise slots, approximately 0.1 mm (0.004 inch) wide, in tough corrosion-resistant material and of maintaining the close slot tolerances necessary during assembly and in flight with associated structural deflections.

A porous surface may also be useful for distributing freezing-point depressant fluid over the wing leading edge and lower surface regions to avoid an accumulation of insects and dirt that could otherwise initiate transition to turbulent flow.

Porous surfaces are not without their own special problems and a number of these are discussed in this paper. However, their potential advantages are sufficient to have encouraged Douglas to investigate

their application for laminar flow control on large commercial transport aircraft. This paper has resulted from that activity.

SYMBOLS

c = wing chord

C_p = pressure coefficient

C_Q = suction coefficient

E_G = Young's modulus for glove panel materials

M_∞ = Mach number

$M_\perp$ = Mach number component normal to sweep

ΔP = pressure drop

R_c = chord Reynolds number

t = airfoil thickness

V = airflow velocity

V_W = average airflow flow velocity through suction surface

V_s = average standard velocity through surface (V_W corrected to sea level conditions)

X_{TR} = transition distance from leading edge

ϵ_{max} = maximum strain

σ_G = stress level in glove panel

Λ = wing sweep angle at 1/4 chord

μ = air viscosity

ρ = air density

POROUS MATERIALS

Based on previous experience (reference 1), four types of fairly smooth porous materials having approximately the right level of porosity were selected for study; Doweave, Fibermetal, Dynapore, and perforated titanium sheet.

The Doweave is woven in three directions from Kevlar fibers. The weave is too open to be used directly as an LFC surface. It was stacked in layers to reduce its porosity and was metallized to increased environmental resistance. The stainless steel Fibermetal is too weak to be self-supporting and was bonded to basic Doweave for added strength. The basic Doweave is shown in figure 2 and the material combinations are shown in figure 3.

Dynapore is a stainless steel woven material that is available in a variety of weaves and gauges. Two grades considered for use as an LFC surface are illustrated in figure 4. Figure 5 shows the 50 x 250 weave photographed at various magnifications using an electron microscope. The flattened surfaces are due to the calendering process which squeezes the woven material to a specified thickness and reduces its porosity. The gaps between the strands can be seen clearly. There are approximately 8700 holes per square centimeter (56,000 holes per square inch) in 80 x 700 and 3900 holes per square centimeter (25,000 per square inch) in 50 x 250 material, as woven.

Figure 6 shows a hole pattern obtained in 0.64 mm (0.025 inch) thick titanium sheet by the electron beam process. The holes are 0.1 mm (0.004 inch) diameter and are spaced 1.0 mm (0.04 inch) apart in both directions. The process is extremely rapid; the hole pattern is preprogrammed and was produced at a rate of about 1200 holes per minute. The rate can be increased up to about 1200 holes per second with thinner sheeting and closer spacing.

Table 1 provides a very rough indication of cost. Some Dynapore weaves are used commercially as filter elements; however, the particular weaves selected were specially produced for Douglas. Perforated titanium and sintered Fibermetal were supplied on an experimental basis only.

No effort was made to project costs on a production basis. However, glove material cost may be put into perspective by considering the $175 per square meter for each LFC surface using a double layer of Dynapore compared with a typical overall wing cost on the order of $6000 per square meter.

SURFACE SMOOTHNESS TESTING

The first step in the selection of porous materials was to test the effective smoothness of alternative surfaces and to determine whether inherent roughness would cause transition. This was investigated on an unswept model with a flat suction surface using the low-turbulence wind tunnel at the Douglas plant in Long Beach.

The model chord was 3.0 meters (10 feet) spanning the 1.37 meter (4.5 foot) tunnel width. It consisted of a flat panel 51 mm (2.25 inch) thick with a sharp wedge section forward and a hinged tapered flap aft. A central pivot allowed variation of the angle of incidence. The porous specimen had a span of approximately 1.2 meters (4 feet) and a chord of 0.3 meter (1 foot). Its leading edge was located approximately 0.6 meter (2 feet) from the leading edge of the model. A plenum chamber beneath the porous specimen was connected to a suction line via a flowmeter and a gate valve to regulate suction. This arrangement is illustrated in figure 7.

The boundary layer was surveyed using a sensor on a hand-held wand. The sensor consisted of a tapered probe with a 1.6 mm (1/16 inch) diameter hemispherical nose covered by a thin platinum film. The film was used as the sensing element of a constant temperature anemometer. The anemometer responded to velocity fluctuation within the boundary layer. The output was amplified

and displayed visually on an oscilloscope and played through a loudspeaker. The audio effect was useful for homing in on the transition region but the visual display was used for more precise location of transition. Typical displays corresponding to various flow conditions are shown in figure 8. Laminar flow is indicated by a low-amplitude oscillation as shown in figure 8A. As the probe is moved downstream, regular peaks may occur as in figure 8B and a constant frequency noise can be heard, sounding rather like a large mosquito. This is caused by the Tollmien-Schlichting small disturbance wave, which has a regular frequency. Further downstream bursts of turbulence can be heard and appear on the oscilloscope as in figure 8C. Further downstream still, the flow becomes completely turbulent as in figure 8D. Transition is judged to have occurred when the turbulent bursts are equal in duration to the intervening laminar conditions. This judgment is noticeably enhanced by the visual display.

SURFACE COMPARISONS

Typical results of transition location are shown in figure 9. The solid symbols identify results obtained with a smooth flat surface at chord Reynolds numbers from 5.2×10^6 to 11.7×10^6. The flat plate transition results are better than those normally expected ($R_{max} = 3 \times 10^6$ from reference 2) due to a favorable pressure gradient obtained upstream of the test specimen. Comparison with the 50 x 250 Dynapore test panel represented by the open symbols in the figure indicates that without suction, there is an initial upstream movement of transition due to inherent surface roughness and the tolerances achieved on the test panel installation. As suction is applied through the surface of the test panel, the transition point moves to a point further downstream than for the flat plate.

Figure 10 compares the transition results obtained at the same Reynolds number with a variety of porous surfaces. Both Dynapore surfaces were more effective than the others at economical low suction flows. The slotted aluminum and the porous titanium panels required much higher suction levels to be as effective. The sintered Fibermetal was less effective than these, and the metallized Doweave was a failure. The 80 x 700 Dynapore surface was clearly the most effective of those tested.

The effect of airflow direction relative to the weave direction for the 50 x 250 Dynapore is shown in figure 11. The surface is less efficient at low suction flows with the airflow at 90 degrees to the weave direction, but even so the coarser Dynapore is still more effective than the alternative surfaces tested.

During tunnel testing with the perforated titanium specimen, it was noticed on two occasions that a particle had become lodged in the surface, causing a turbulent wedge to appear. Laminar flow was restored by rubbing the surface smooth without removing the blockage, thus proving that transition had been caused solely by the protrusion of the particle above the surface. These conditions were not experienced during any of the testing with the Dynapore specimens.

The relative merits of alternative suction surfaces when subjected to cross flow conditions still need to be evaluated using a swept wing wind tunnel model. Flight testing would be necessary to obtain fully representative conditions at high Mach numbers combined with high Reynolds numbers.

Typical pressure distributions for airfoils suitable for laminar flow are shown in figure 12. For a swept wing, suction requirements increase in the regions of steep pressure gradients that occur both near the leading edge and aft of approximately 60 percent chord. This is reflected in the suction flow velocity requirements for the upper and lower surfaces, as shown in figures 13 and 14.

Outflow through the surface must be avoided as it would destroy laminar flow. Suction pressure below the surface must therefore be less than the lowest pressure over any external surface area that is connected to a common plenum or local duct region. This requirement defines the minimum pressure drop allowable through the surface. A typical value is 0.013 of the free-stream dynamic pressure for the upper surface of the glove panel in the main structural box region. For a flight condition of Mach 0.8 at 12,190 meters (40,000 feet) altitude, the minimum pressure drop through the surface would be 110 Pa (2.3 lb/ft^2) with a velocity of 0.03 m/sec (0.1 ft/sec). Most of the flow resistance within the glove panel is supplied by the porous surface material itself, but there is additional resistance in the backing material and flow channels.

SUCTION CHARACTERISTICS

Typical flow rates versus pressure drop for the suction surfaces compared previously are shown in figure 15. It is interesting to note that the Dynapore material retained a straight-line relationship with the pressure drop directly proportional to the velocity as indicated by the 45-degree slope, whereas this relationship varied for the other materials. For the slotted surface, for example, the pressure drop changed from being proportional to V_S toward a V_S^2 relationship at the higher velocities. All of these surfaces were more open than that required, as illustrated.

Since both suction velocity and surface pressure drop requirements increase with increasing external pressure gradients (either positive or negative), the required porosity envelope tends to follow a ΔP versus V_S relationship similar to that of the porous materials themselves. This characteristic should allow a porous surface with a single level of porosity to cover a fairly wide range of external pressure conditions. Methods of varying porosity were next considered, with particular reference to the Dynapore materials that were shown previously to have the most promising surface characteristics.

POROSITY REDUCTION

The effective porosity for perforated or slotted surfaces can be modified by changing hole size and distribution or slot width and spacing, respectively.

The possibilities for reducing porosity on Dynapore woven materials include the following: (1) varying the fiber thickness and weave; (2) increasing the calendering (or squeezing) of the material after weaving; (3) adding metering layers beneath the surface layer, (4) plating the fibers after weaving, and (5) blocking the porosity.

Figure 16 shows the effect of calendering on 50 x 250 and 80 x 700 weaves. For a single layer, considerable squeezing is necessary for either weave to reduce porosity to the useful range indicated. Too much calendering reduces the strength of the individual fibers by introducing severe stress raisers, particularly from the aspect of fatigue. The necking of the fibers is illustrated in figure 17. To retain acceptable strength characteristics, the amount of squeezing is being limited to no more than 40 percent.

The addition of metering layers may not bring about as rapid a reduction in porosity as might be expected. Increasing the number of porous metering plies sandwiched between relatively open Doweave layers was found to result in a diminishing effect. The pressure drop, with as many as five intervening layers, was still well below the desired level and increasing the number of layers further had little effect.

Plating may be used to reduce porosity but with the triangular-shaped pores in Doweave measuring only 0.043 mm by 0.02 mm (0.0017 by 0.0008 inch), the plating process would need to be very carefully controlled.

During early experiments, the bonding adhesive wicked and spread very badly on one specimen of 50 x 250 Dynapore bonded to a honeycomb cell backing; this is shown in figure 18. In effect, the specimen was surfaced with a regular pattern of porous holes with random nonporous areas superimposed. To our surprise, the surface performed satisfactorily in the tunnel. A comparison with the results obtained on an unblocked 50 x 250 panel is shown in figure 19. This encouraging result indicated that porosity could be satisfactorily reduced by intentional blocking. Two possibilities were considered: (1) blanking off large continuous areas to create a porous strip effect, and (2) using a perforated sublayer to obtain a distributed blanking effect. Both methods offer the additional advantage of an opportunity for varying porosity levels within a single panel.

Figure 20 gives the dimensions of a porous strip panel that was tested. The static flow characteristics are shown in figure 21. As indicated, the porosity moved into the desired range and the pressure drop remained directly proportional to the velocity.

The laminar flow performance of the porous strip configuration (figure 22) is better than for the original 50 x 250 panel for low-suction flows. This is probably due to reduced surface roughness as indicated by the increased extent of laminar flow obtained with porous strips compared with the unblocked specimen, with suction off.

Various hole patterns are currently under consideration for the perforated sublayers.

SURFACE IMPACT RESISTANCE

A further consideration with respect to surface sublayers is impact resistance. The Dynapore is woven in a softened condition and is work-hardened to some extent during the calendering process. However, it is still too soft to be used at the outer surface without some reinforcing. A perforated fiberglass sublayer used to partially block the porosity can also be used to provide increased impact resistance.

As an aid to bonding the 80 x 700 Dynapore surface to the fiberglass sublayer and to improve strength accross the perforations, an additional layer of 80 x 80 Dynapore may be interposed between them and diffusion-bonded to the outer surface layer. Penetration of resin into the more open weave results in a stronger bond between the Dynapore and the fiberglass layers. Figure 23 shows an 80 x 80 sublayer diffusion-bonded to an outer 80 x 700 surface.

Test results indicate that by adding the perforated glass laminate under the Dynapore, it should be possible to provide a surface with adequate impact resistance for the main box area. As a repair procedure for any accidental dents that may occur in the surface, local filling, even with the resulting blocking of the porosity, may be satisfactory due to the apparent insensitivity of the laminar flow performance to local blockage. This would not be acceptable, however, if a cratered lip were to occur around a large dent, as was experienced before introducing the reinforcing sublayer. The initial design aim would be for impacts up to 5.65 N-m (50 lb-in.) to be quickly repairable by filling, if necessary.

STRAIN COMPATIBILITY

A major consideration for glove panel design is strain compatibility with the main load-carrying structure because the glove must strain with the structure to avoid surface gaps. Primary structural materials with a high ratio of stiffness to usable strength are therefore advantageous. Figure 24 illustrates this factor for a number of primary structural materials. Of the materials considered, graphite/epoxy composite structure would be the most compatible, aluminum second, and titanium last from this point of view.

In addition to structural loads, differential thermal expansion stresses must be taken into consideration. By subtracting the thermal strain that could be induced in the glove from the total strain available, the strain remaining for structural loads can be obtained.

The combined effect of structural and thermal strain for a number of material combinations is shown in table 2. The table shows that a Dynapore surface supported by a fiberglass sandwich panel should be compatible with all of the primary structural materials considered.

LFC GLOVE PANEL DESIGN

The selected glove panel design is based on the Lockcore* principle. This construction was developed primarily for use as a noise-damping panel for engine air inlets; it is illustrated in figure 25.

Figure 26 shows how the Lockcore principle can be applied to a laminar flow control panel. It provides a porous LFC surface and internal suction flow collector ducts and could have adequate impact resistance, strength, and stiffness. With LFC on, air is sucked from the boundary layer through the diffusion-bonded Dynapore layers and the supporting perforated fiberglass layer. It then passes through the outer porous fiberglass layer of the supporting sandwich panel and flows into channels formed by the fluted stiffeners.

To avoid not having suction for more than a short distance along the flow direction within the boundary layer, all suction flow discontinuities including panel joints may be inclined across the flow direction. The glove panel stiffeners may also be included parallel with the panel joints, as illustrated in figure 27.

GLOVE PANEL AND WING STRUCTURE COMBINED

The LFC suction glove panel is attached to the integral blade stiffeners of the primary wing box structure, as illustrated in figure 28. The figure shows how suction air flowing within the Lockcore panel is transferred to collector channels ending in adjustable nozzles that control the flow into each main spanwise integral duct formed by blade stiffeners on the main load-carrying panel. The flow channels within the Lockcore panel are blocked in line with each main stiffener. This limits the effect of external chordwise pressure variations and allows pressure drop requirements through the surface to be kept small. The integral ducts run closely parallel with the wing isobar pattern: this also helps to reduce pressure drop requirements along the duct. The collection channels and adjustable nozzles are an integral part of the glove panel. The nozzles can therefore be preset on the bench to meet the required flow values and to compensate for any variations in panel porosity. This is a considerable advantage in initial assembly and maintenance.

*Lockcore is a Douglas patent process.

By using removable porous glove panels surrounding the basic wing structure, further advantages arise, which include the following:

1. Choked or damaged panels could be removed and cleaned or replaced without disturbing the primary wing structure.

2. A smooth external surface matching the airfoil profile is not a requirement for the basic structure. Hence, joints, attachments, doublers, and any repairs or modifications of the basic structure may be simplified.

3. The removable glove suction panels do not have to meet the same fatigue life requirements as the primary wing structure.

4. The main structural box, integral ducting, and systems are accessible for inspection, maintenance, and repair, by removing the glove panels, and manholes can be provided in the primary structure to gain access to fuel tanks in the normal manner without conflicting with the suction system.

5. With external blade stiffeners, the main structural box benefits from a smooth interior surface. This simplifies rib design by avoiding stiffener cutouts, and simplifies the diffusion of concentrated loads into the main box shell. Trapped pockets of unusable fuel are also avoided.

CONTAMINATION AVOIDANCE

The remains of any insects impacted on the surface exceeding a height of about 0.1 mm (0.004 inch) are likely to cause transition followed by a wedge of turbulent flow on the surface. One way of avoiding this situation that has been tested on a Jetstar airplane is to ensure coverage of the impact region with a continuous fluid film during the period of exposure to insects.

A porous surface offers the possibility of providing fluid coverage over critical areas by using porous strips for fluid distribution. Fluid flowing back across a smooth surface has a tendency to collect into rivulets. This could leave the surface between the rivulets exposed to contamination. Tunnel testing with fluid flowing back on porous surfaces, however, has shown that once the porous surface is wet, there is no longer a tendency to form rivulets. This suggests that for a porous surface, the high rate of flow necessary to wet the surface could be reduced subsequently to a more economical level.

A difficulty is caused by the movement of the stagnation point around the leading edge during takeoff and climb. Because the fluid could not flow against the airstream, it may be necessary to distribute fluid through the surface over the entire stagnation region to ensure complete coverage.

Testing also showed that a porosity suitable for laminar flow control would result in excessive fluid flow in order to maintain an even distribution. Therefore, either a higher pressure drop through the surface would be needed or the fluid flow would need to be pulsed at intervals. The latter alternative would be more consistent with the requirement for wetting the entire surface initially.

Freezing point depressant (FPD) type fluid would be required for the anticontamination system, and this could also be used for de-icing.

CONCLUDING REMARKS

The results of Douglas studies to date support the use of porous materials to achieve laminar flow. Various porous materials have been considered for application to LFC wing surfaces, and four candidate porous surface materials have been subjected to a series of screening evaluations with the following results:

Laminar flow tests with suction, which account for Tollmien-Schlichting instabilities but not cross-flow instabilities, indicate that all but one of the surfaces tested are sufficiently smooth. Of these, fine mesh Dynapore requires far less suction to substantially extend the region of laminar flow than the other surfaces, including a slotted one.

The LFC performance of the Dynapore surfaces is not affected by locally blocked regions and the overall porosity may be tailored to meet LFC requirements by controlled blockage that can produce porous strips or porous hole patterns.

Dynapore surfaces perform satisfactorily with the weave in either direction relative to the flow, but perform better with the airflow at 90 degrees to the warp.

The impact resistance of a Dynapore surface is inadequate without backup layers that may also be used to moderate porosity.

Tests indicate that the porous surface could be used with fluid systems for the prevention of contamination and icing.

A possible LFC suction glove arrangement has been identified with material combinations compatible with thermal expansion and structural strain.

REFERENCES

1. Development of Technology for the Fabrication of Reliable Laminar Flow Control Panels on Subsonic Transports. NASA CR-145125, October 1976.

2. Schlichting, Hermann: Boundary Layer Theory. McGraw Hill, 1968.

TABLE 1

LFC SURFACE MATERIALS COSTS

MATERIAL	APPROXIMATE COST ($/m^2)	
	SINGLE PLY	FOR EQUAL ΔP
• METALLIZED DOWEAVE[2]	116	231[1]
• SINTERED FIBERMETAL	646[2]	770[1][3]
• DYNAPORE		
50 x 250	113	113
80 x 700	133	133
80 x 700/80 x 80	175	175
• PERFORATED TITANIUM	1884[2]	1884

[1] MULTIPLE LAYERS — BONDING COST EXCLUDED

[2] EXPERIMENTAL QUANTITY

[3] SUPPORTED BY DOWEAVE

TABLE 2

COMPATIBILITY OF MATERIALS (STRUCTURAL PLUS THERMAL STRAINS)

FEASIBLE COMBINATIONS		
	PANEL MATERIAL	STRUCTURE MATERIAL
SINGLE MATERIAL PANELS	316L DYNAPORE KEVLAR/EPOXY GLASS/EPOXY	GRAPHITE BORON ALUMINUM TITANIUM
MULTIMATERIAL PANELS	50 x 250 + KEVLAR	GRAPHITE BORON ALUMINUM
	50 x 250 + GLASS	GRAPHITE BORON ALUMINUM TITANIUM

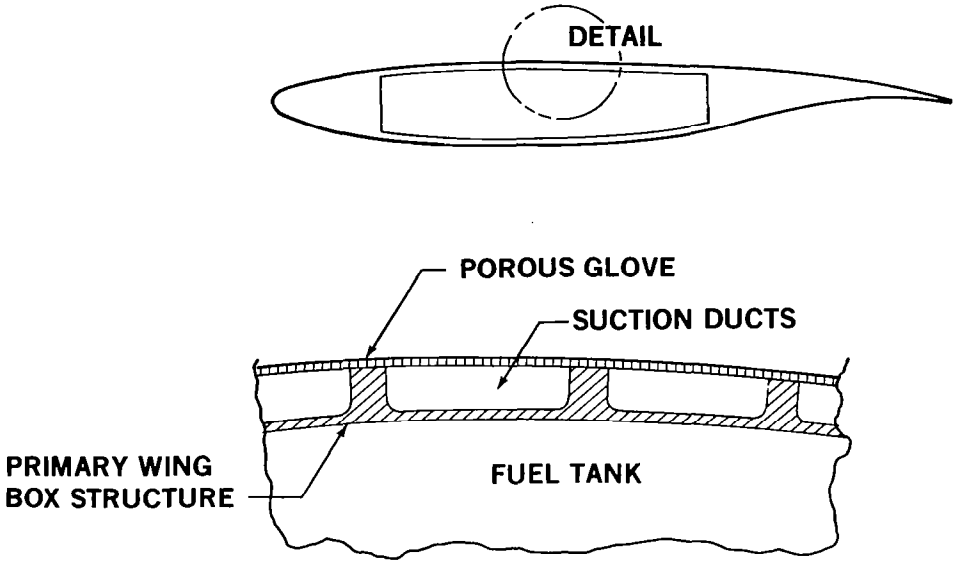

Figure 1.- LFC porous suction glove.

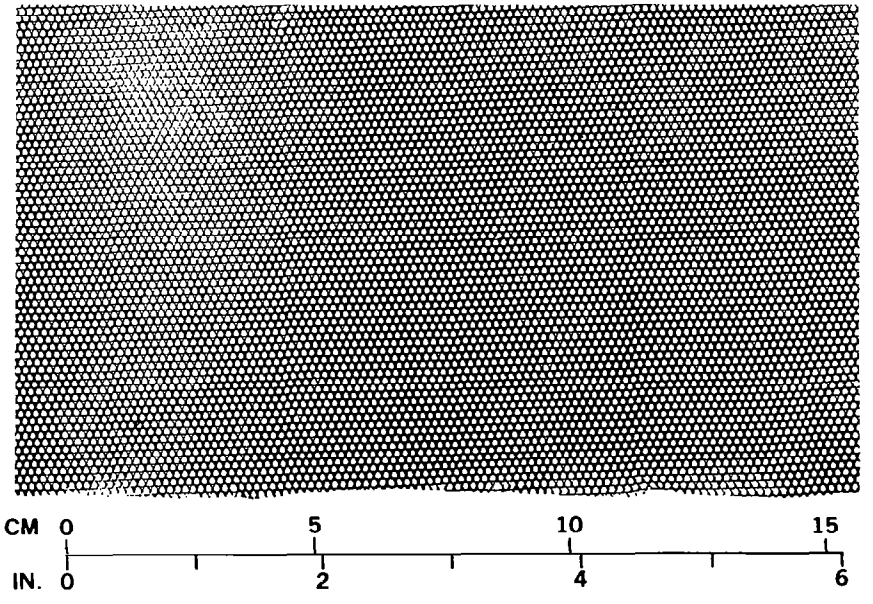

Figure 2.- Basic Doweave.

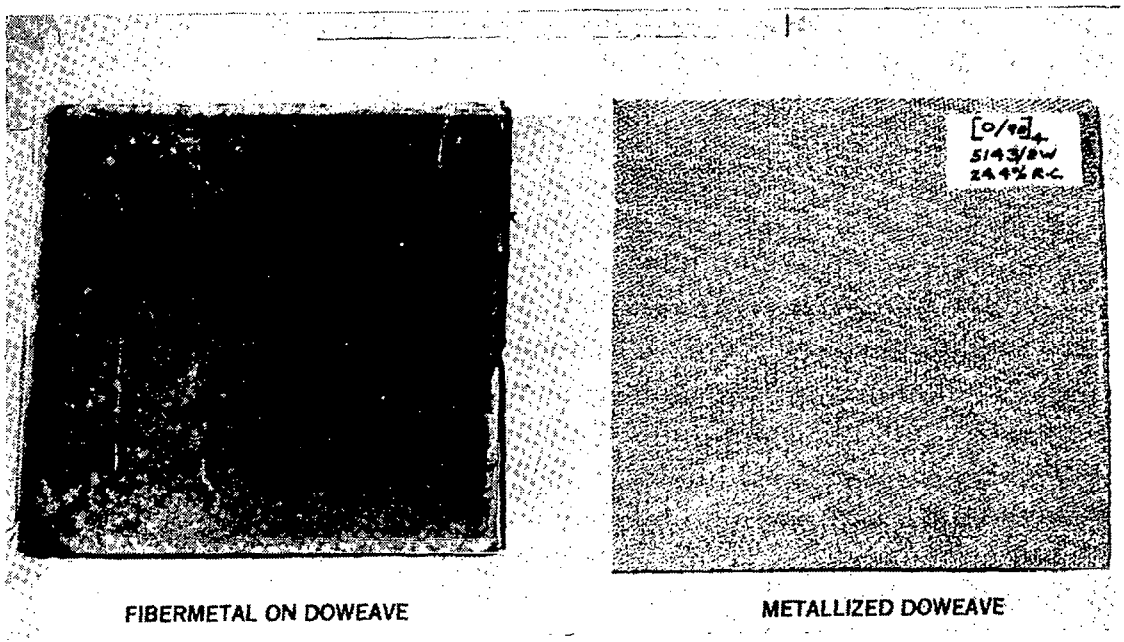

Figure 3.- Porous surface samples.

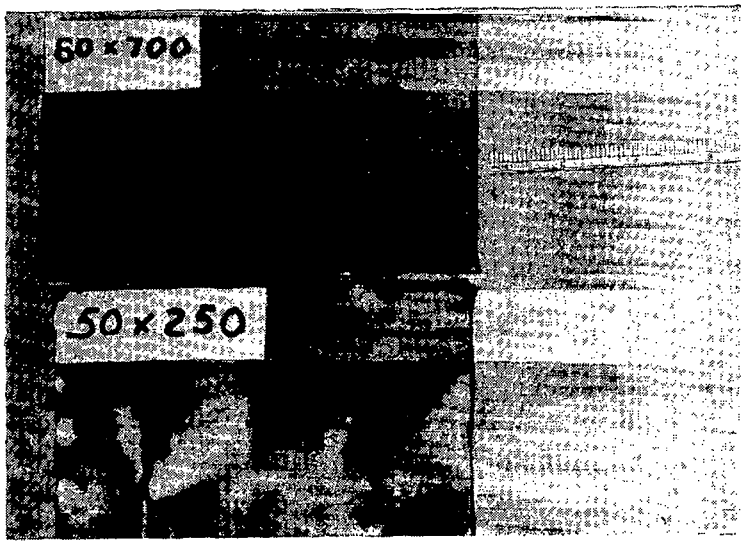

Figure 4.- Dynapore surfaces.

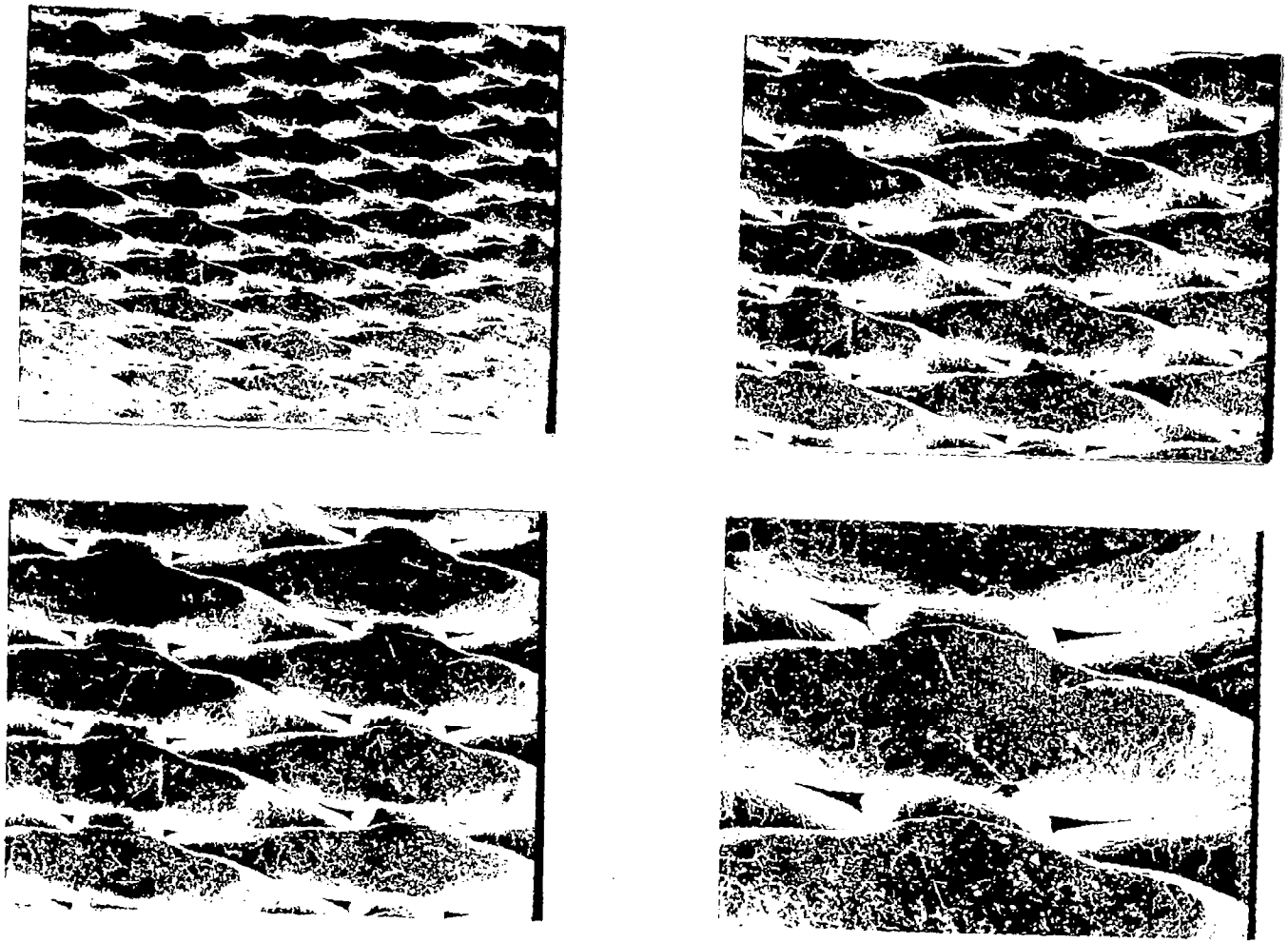

Figure 5.- 50 × 50 Dynapore surface englarged (40× to 200×).

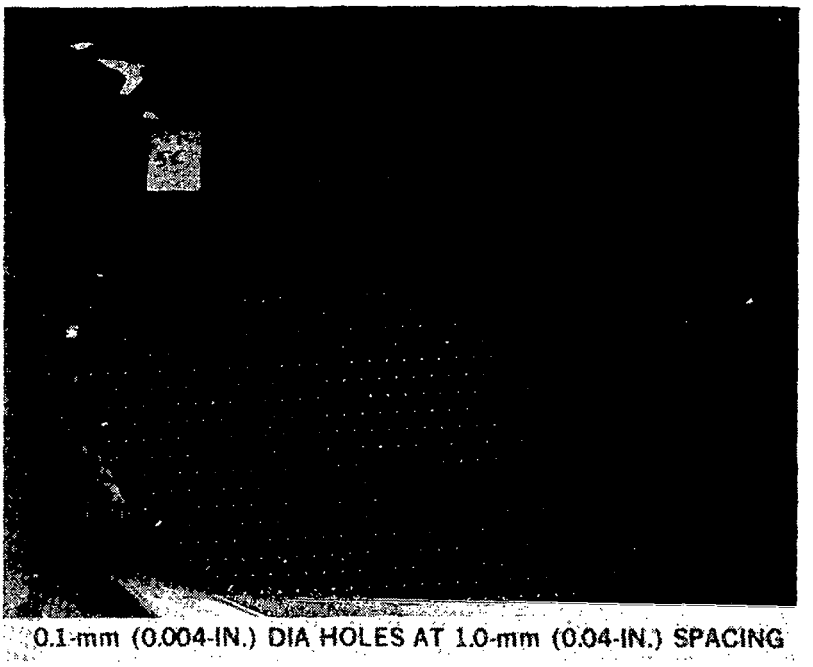

Figure 6.- Electron beam perforations in titanium sheet.

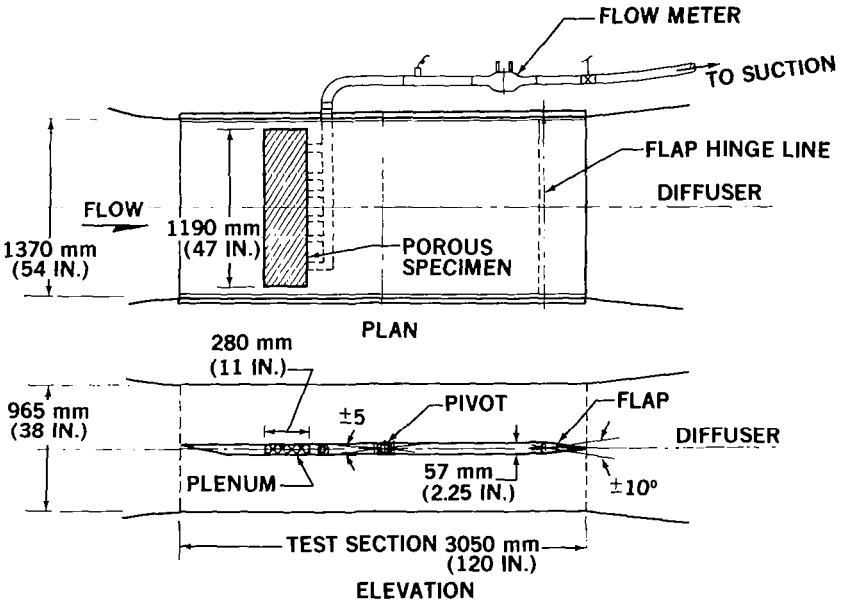

Figure 7.- Wind tunnel model test for laminar flow with porous surface specimens.

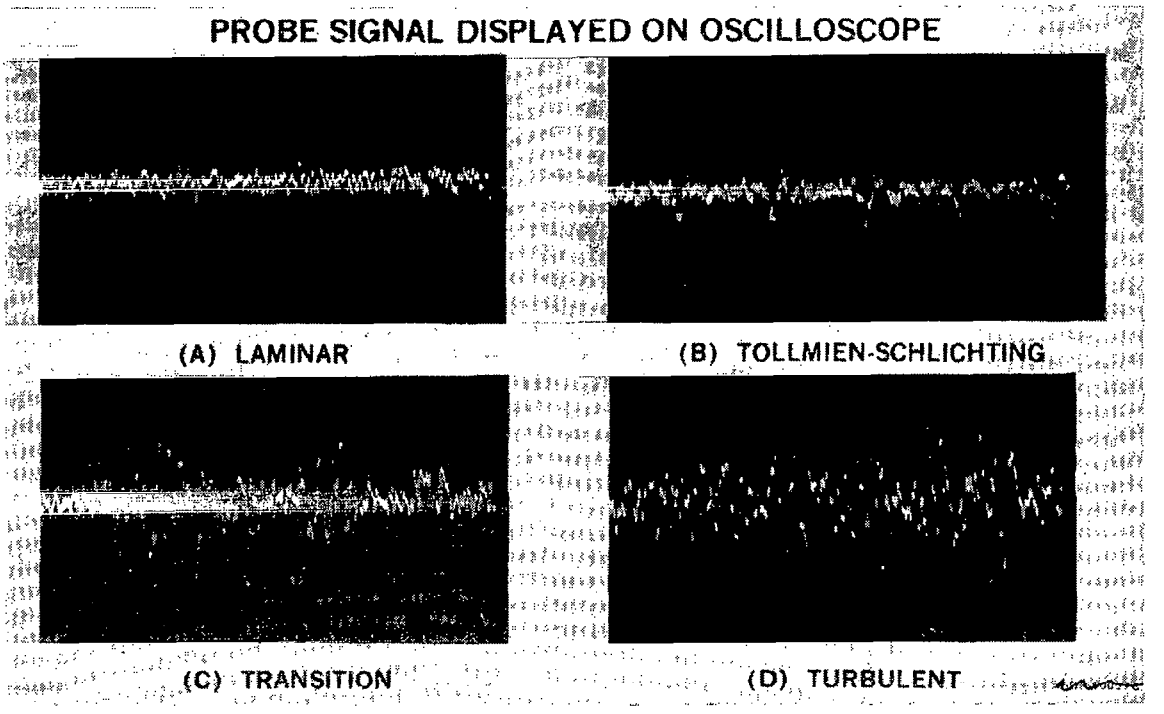

Figure 8.- Boundary-layer signatures.

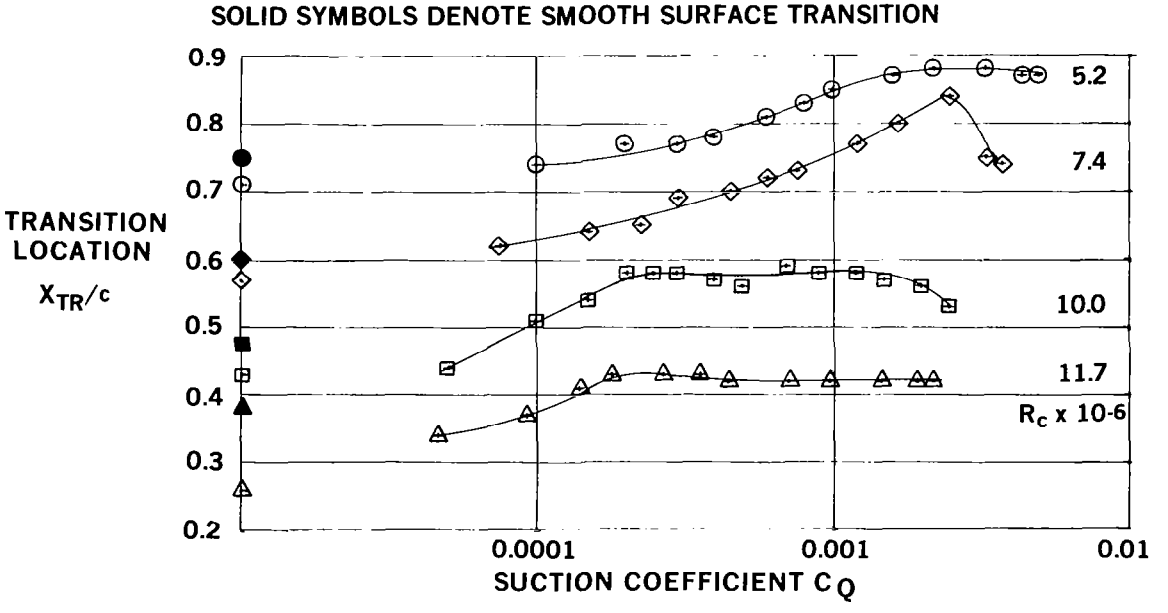

Figure 9.- Typical results — transition location, 50 × 250 Dynapore surface.

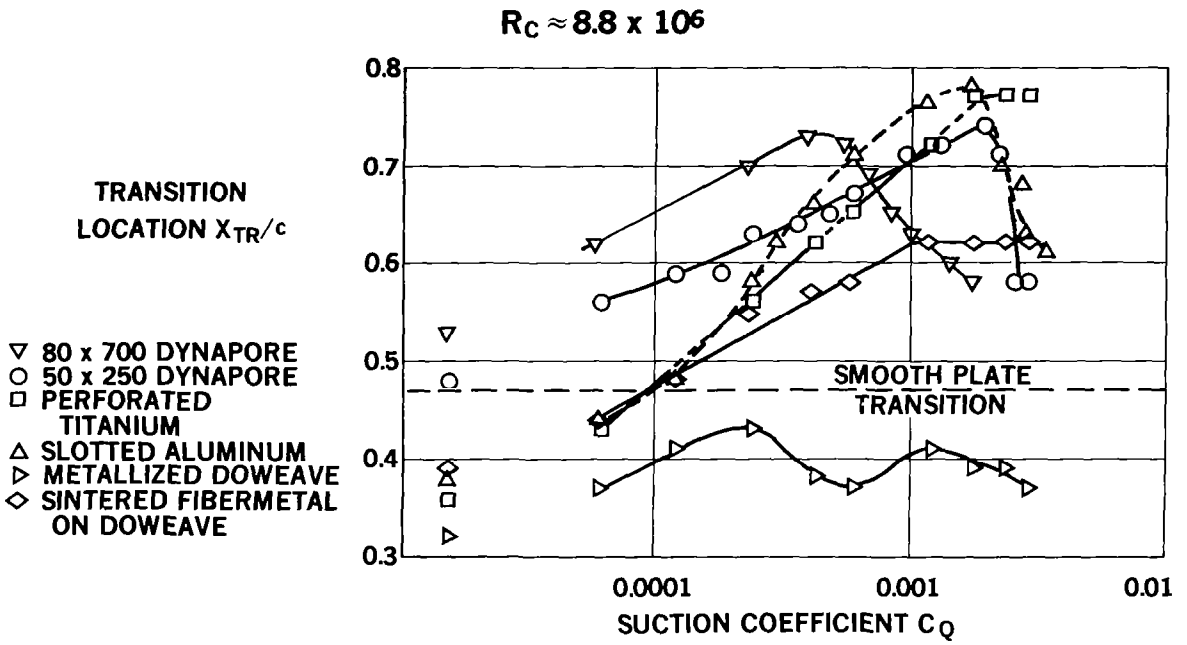

Figure 10.-Comparative effectiveness of laminar flow control surfaces.

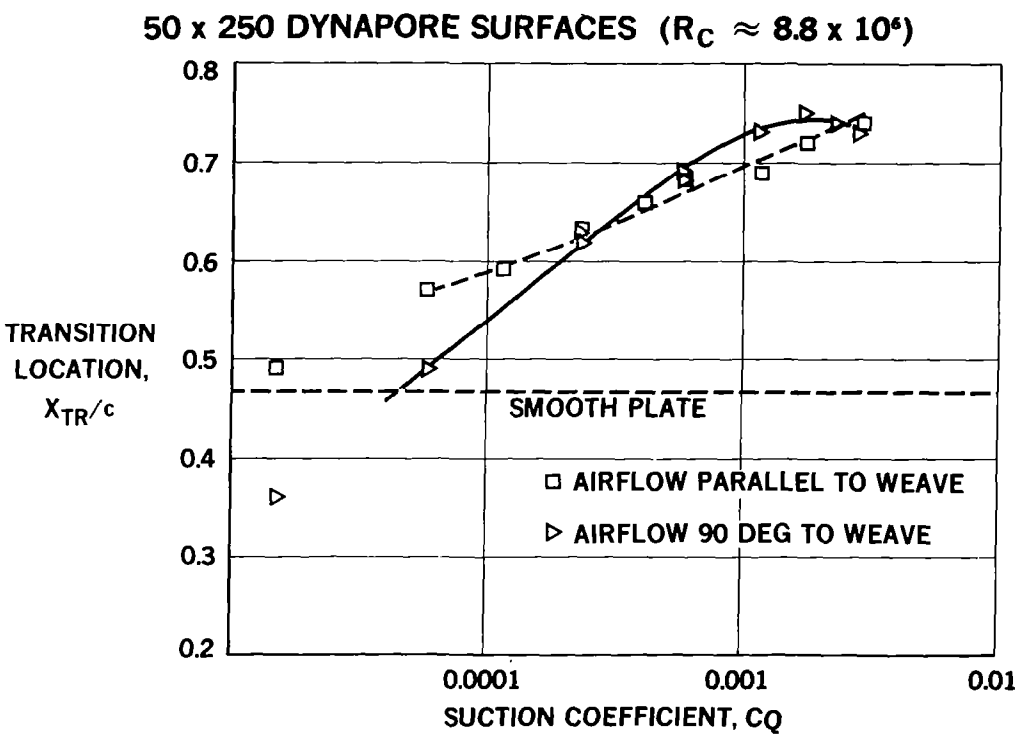

Figure 11.- Effect of airflow direction relative to weave.

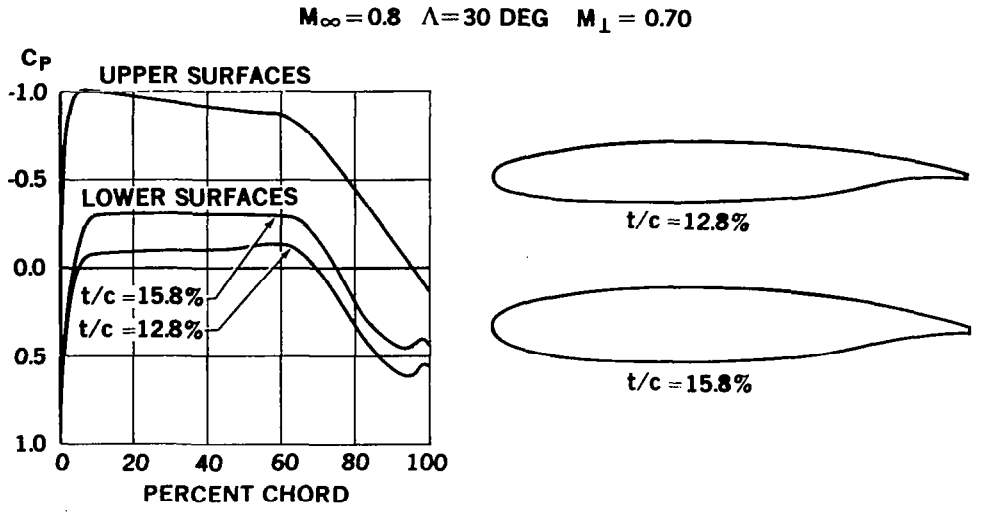

Figure 12.- Typical design pressure distributions and airfoil shapes.

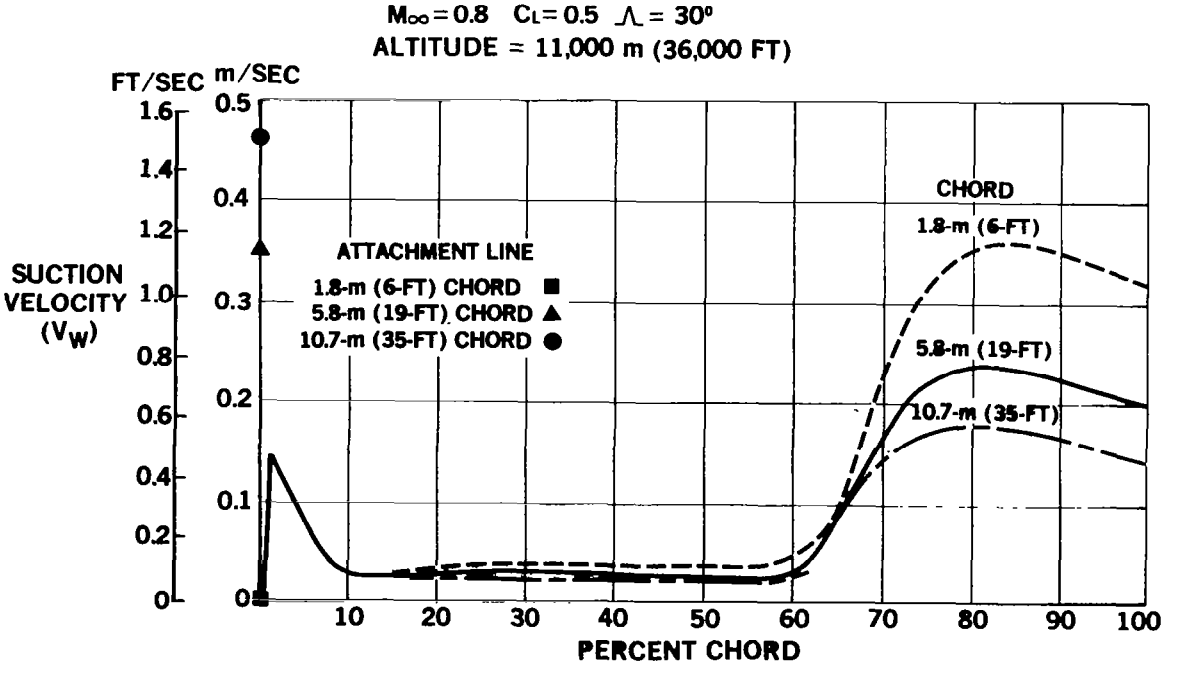

Figure 13.- Typical suction distributions — upper surface.

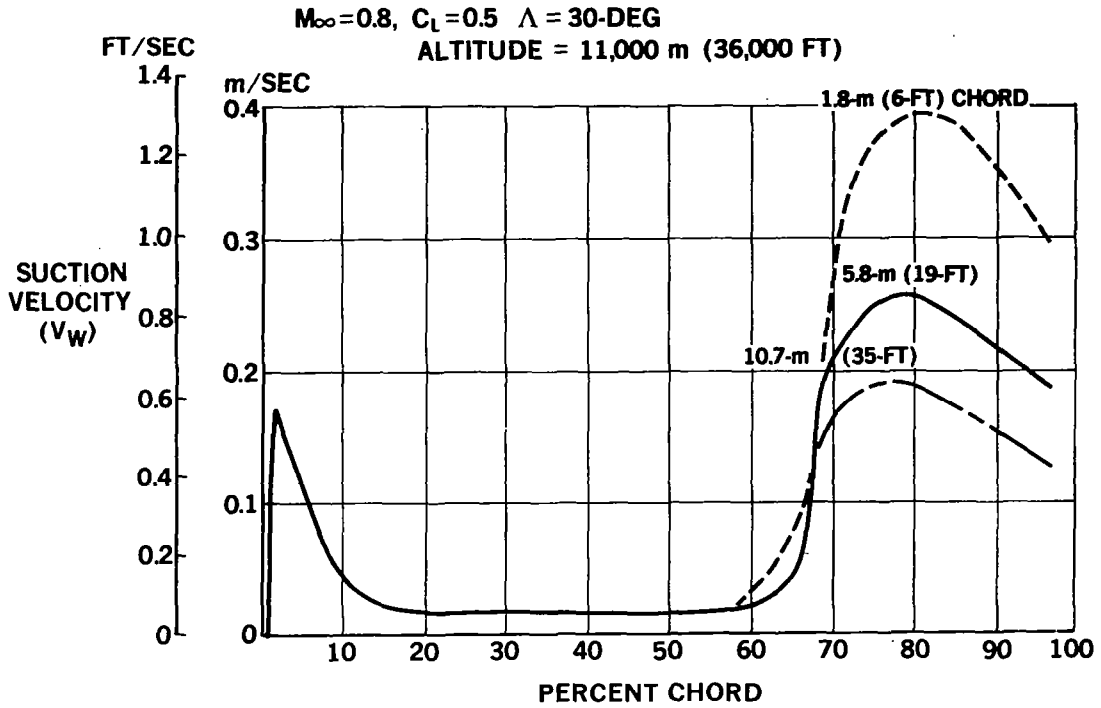

Figure 14.- Typical suction distributions — lower surface.

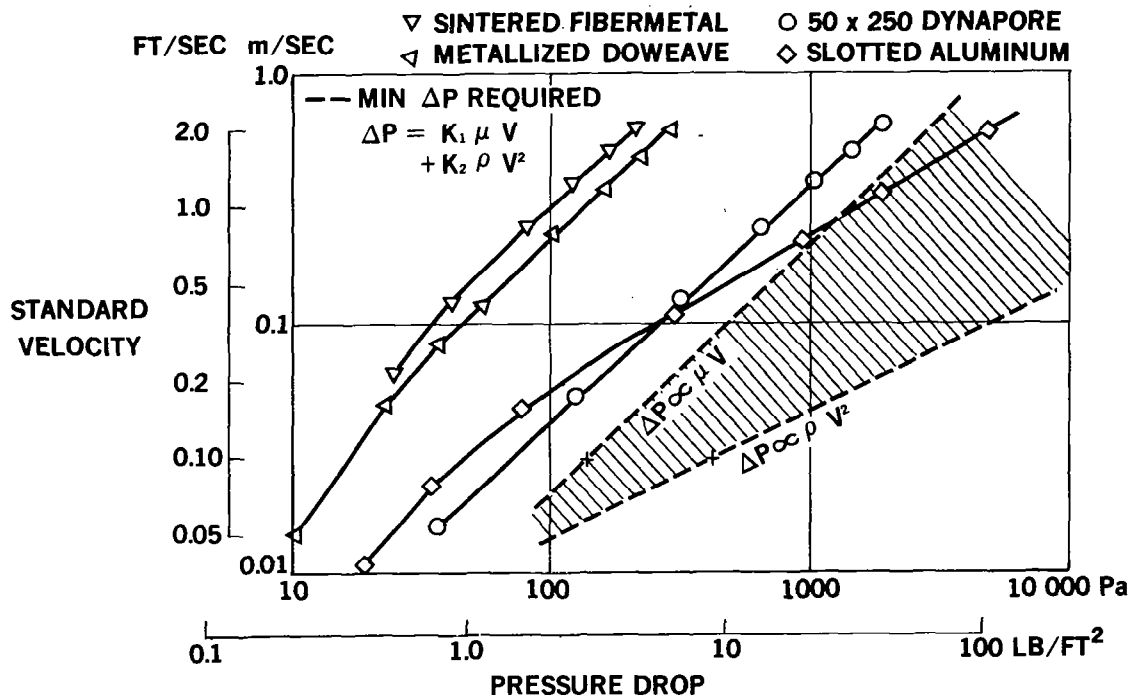

Figure 15.- Comparative static flow characteristics (sea-level test).

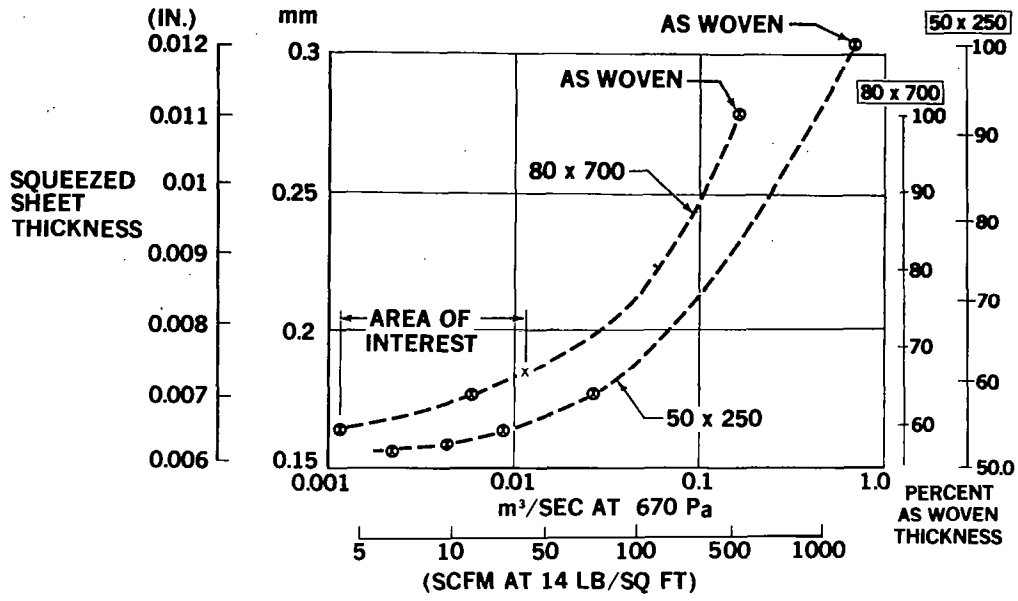

Figure 16.- Effect of calendering on porosity of Dynapore materials.

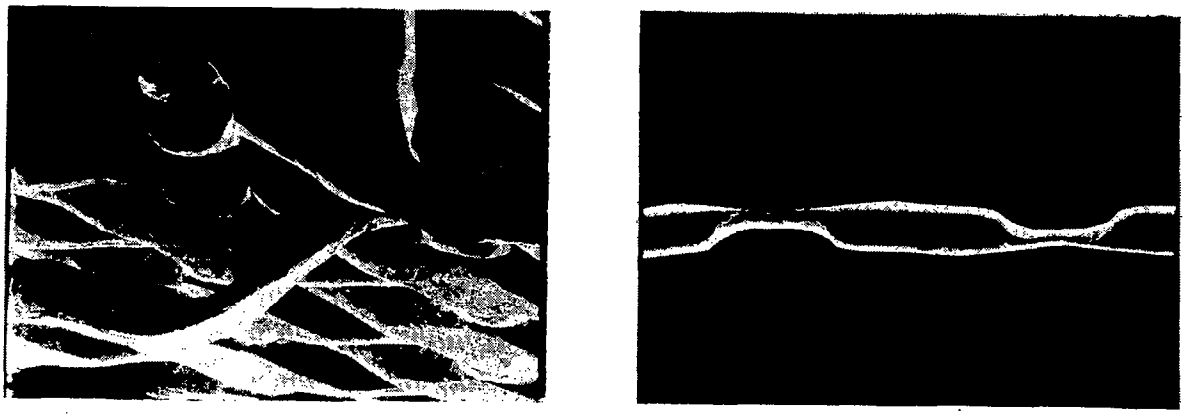

Figure 17.- Effect of oversqueezing Dynapore during calendering process.

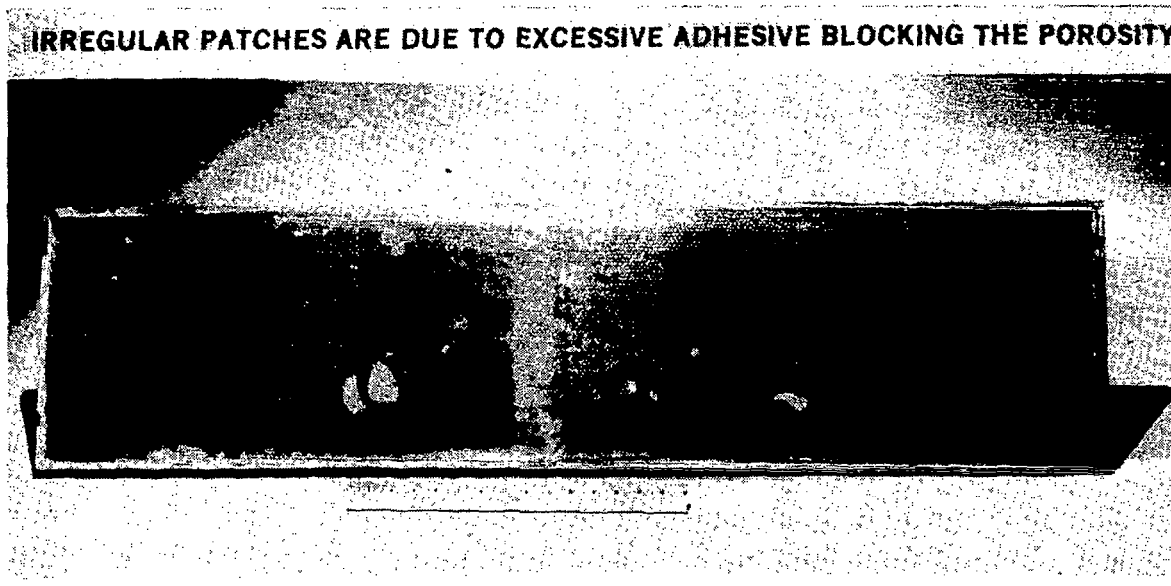

Figure 18.- 50 × 250 Dynapore-honeycomb sandwich — adhesive blocking porosity.

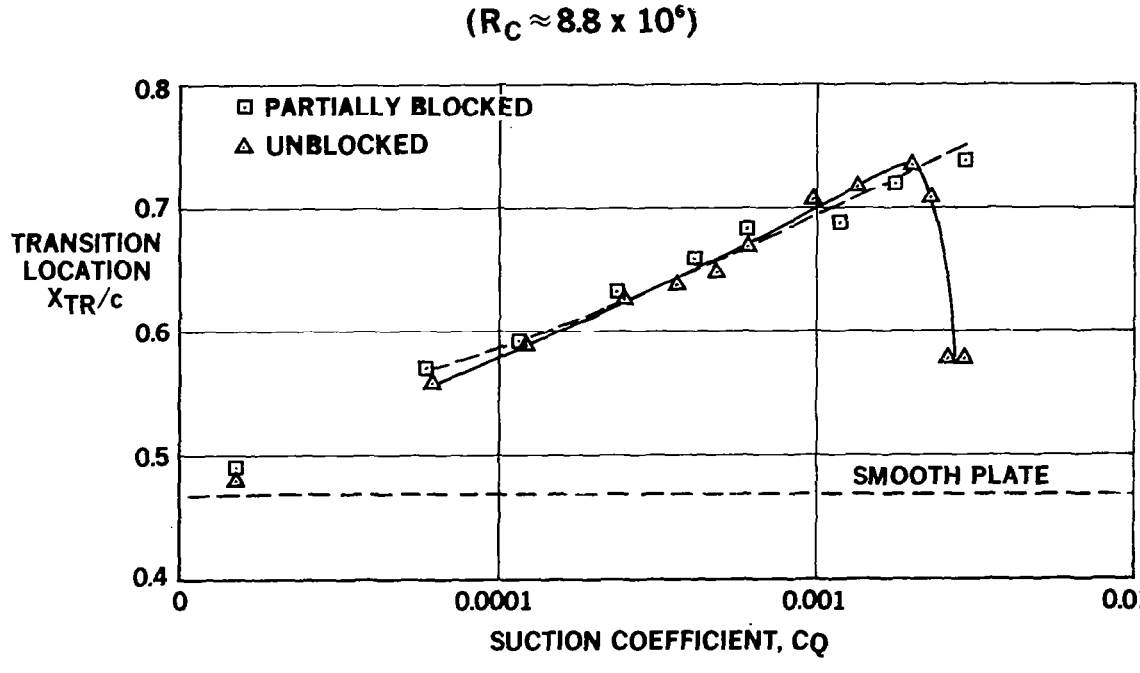

Figure 19.- Porosity blockage effect on 50 × 250 Dynapore surfaces.

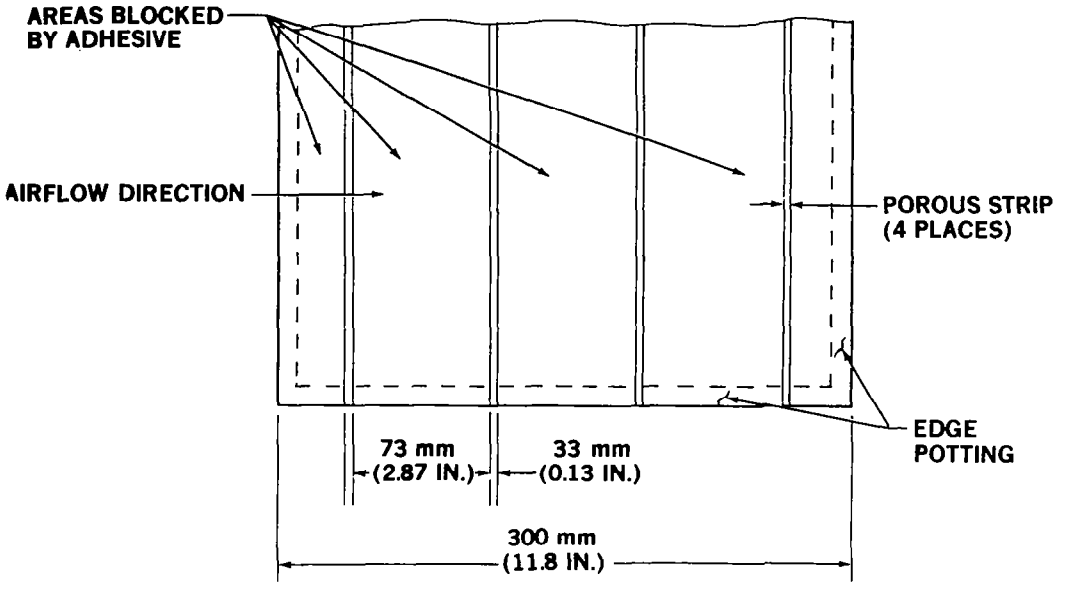

Figure 20.- Porosity strip test panel.

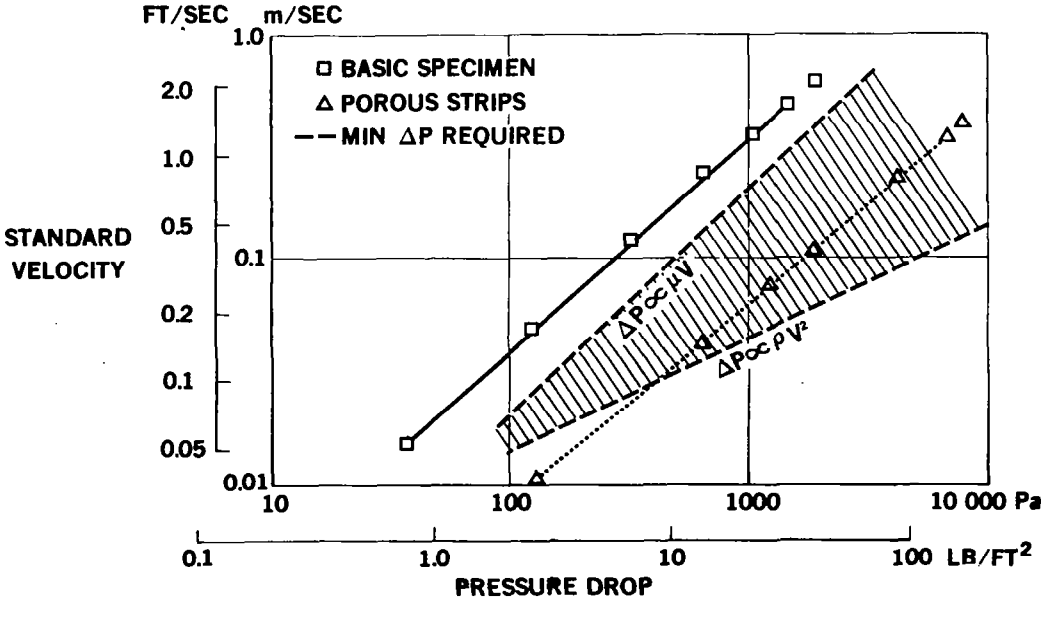

Figure 21.- Porous strip static flow comparison, 50 × 250 Dynapore.

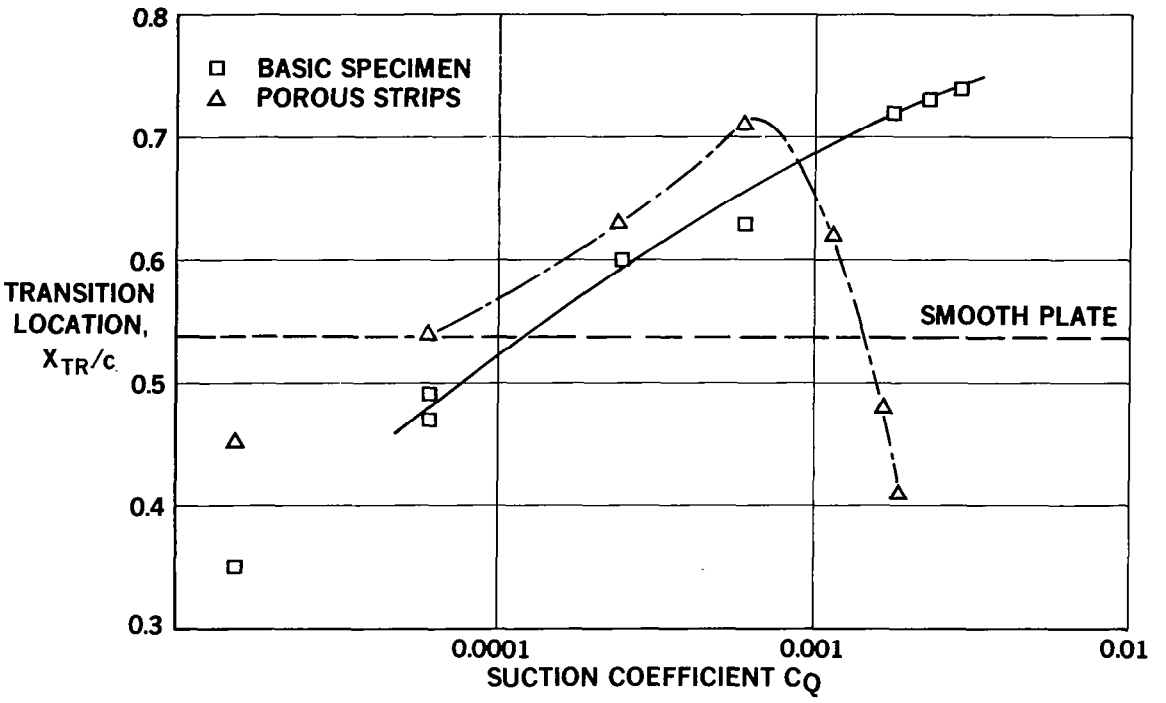

Figure 22.- Porous strip LFC performance comparison, 50 × 250 Dynapore.

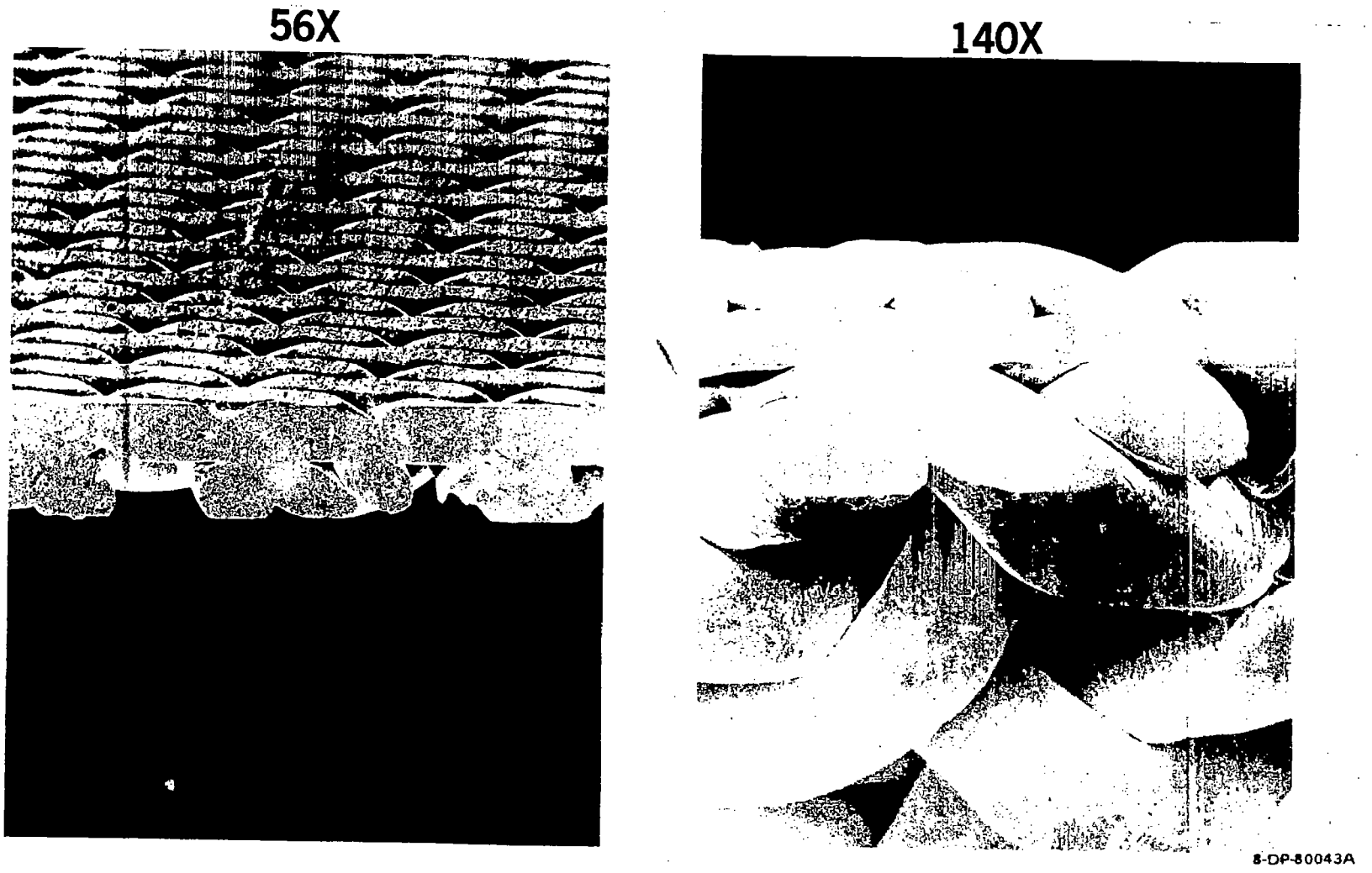

Figure 23.- 80 × 700 Dynapore surface plus diffusion-bonded 80 × 80 sublayer.

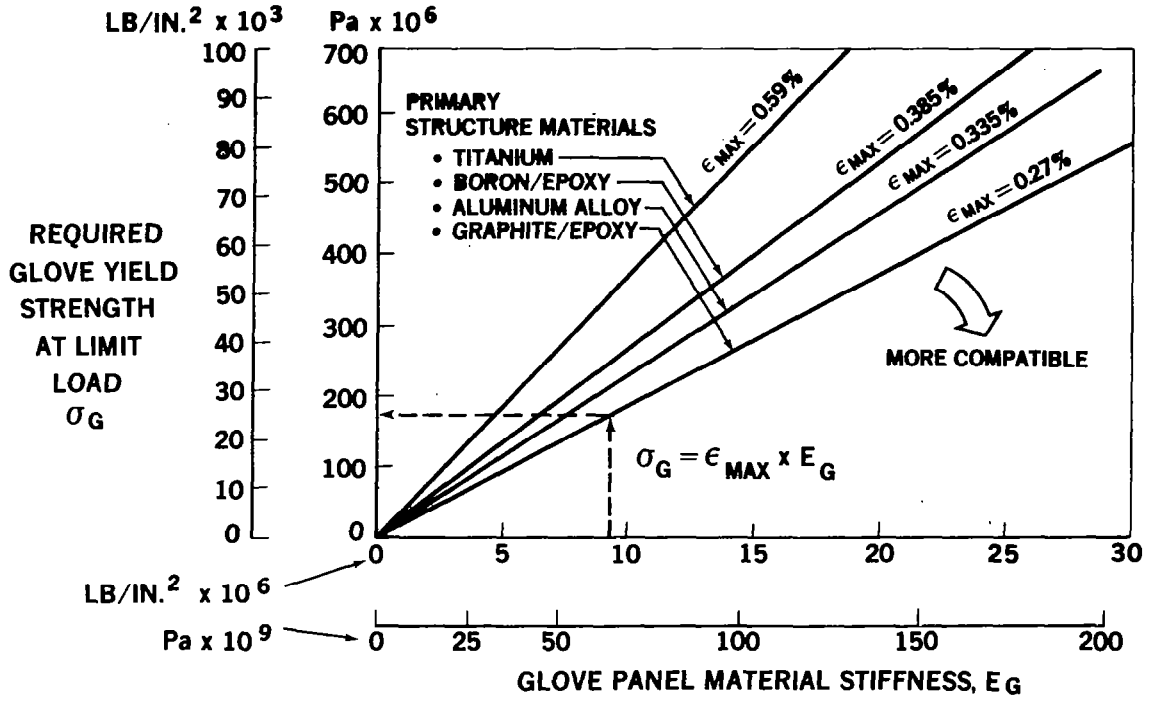

Figure 24.- Glove strength required to match structural strain.

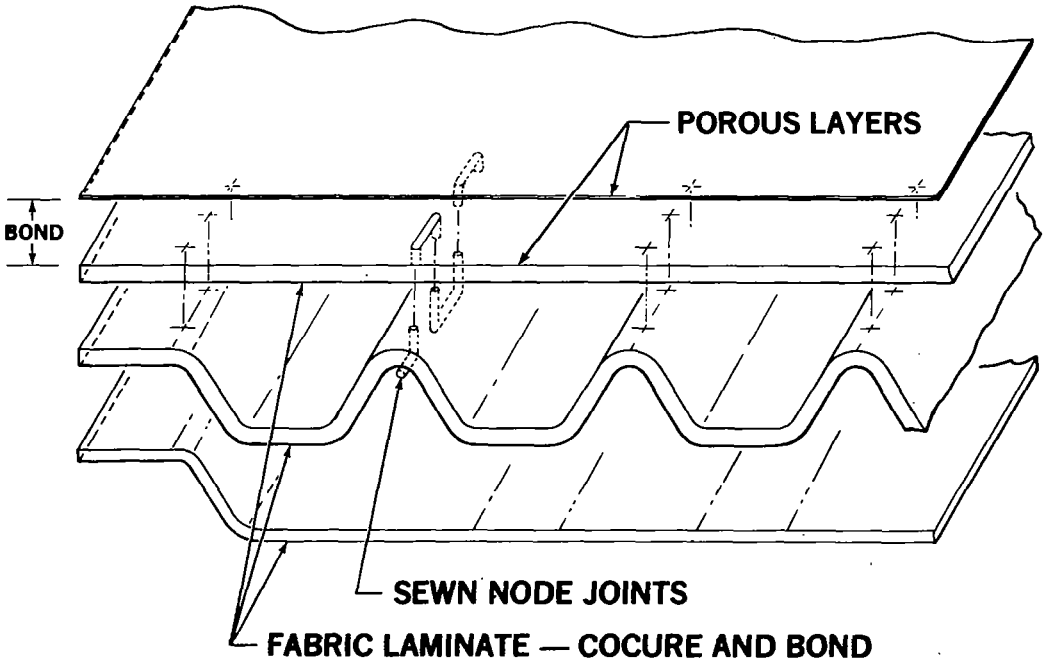

Figure 25.- Typical Lockpore panel construction.

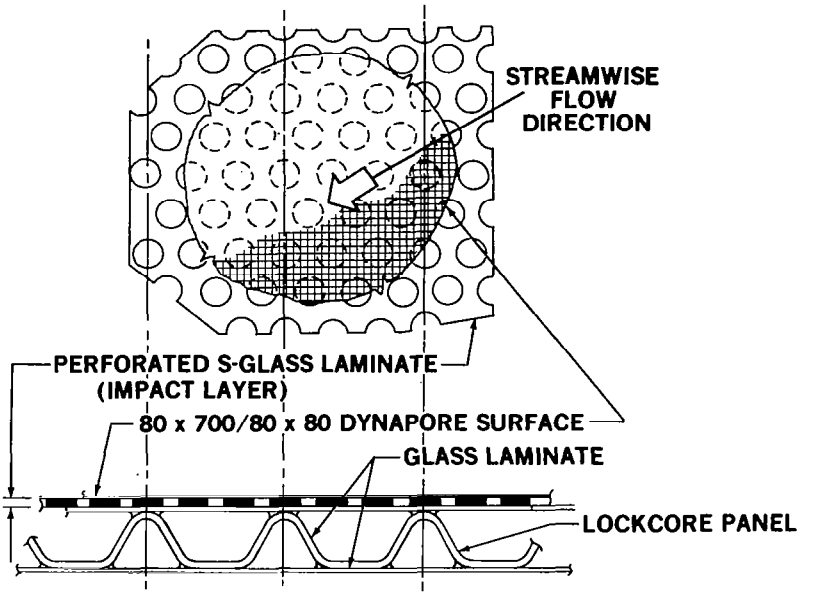

Figure 26.- Glove panel with perforated fiberglass sublayer.

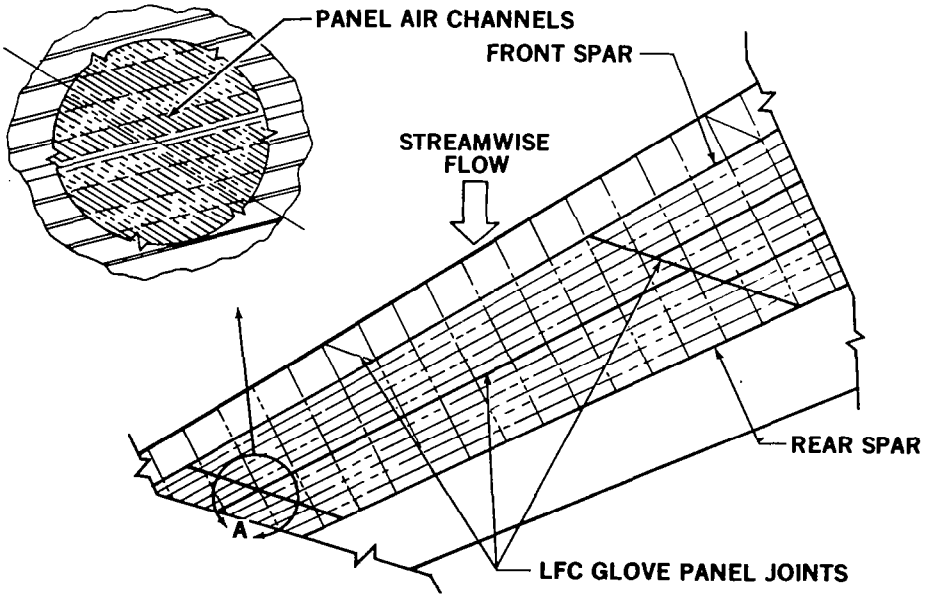

Figure 27.- Typical wing box glove panel arrangement.

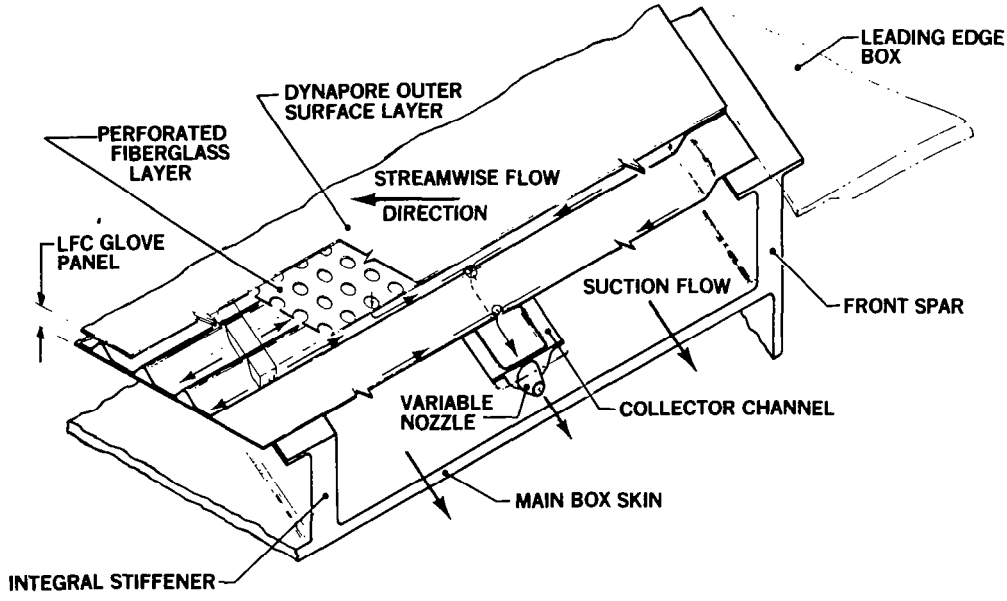

Figure 28.- Gloved wing structural concept.